CUL7: A DOC domain-containing cullin selectively binds Skp1·Fbx29 to form an SCF-like complex

Dora C. Dias*, Georgia Dolios†, Rong Wang†, and Zhen-Qiang Pan*‡

*Derald H. Ruttenberg Cancer Center and †Department of Human Genetics, Mount Sinai School of Medicine, One Gustave L. Levy Place, New York, NY 10029-6574

Communicated by Jerard Hurwitz, Memorial Sloan–Kettering Cancer Center, New York, NY, October 24, 2002 (received for review September 3, 2002)

Selective protein degradation targeted by members of the F-box protein family plays pivotal roles in cell biology. It is widely accepted that an F-box protein directs substrate ubiquitination within a Skp1·CUL1·F-box protein·ROC1 (SCF-ROC1) E3 ubiquitin ligase complex. This assembly utilizes the CUL1 molecular scaffold, allowing the F-box protein to position its bound substrate for ubiquitination by a ROC1-recruited E2-conjugating enzyme. Here, we describe an alternative mechanism for assembling an F-box protein-based E3 complex through a previously uncharacterized cullin, CUL7, identified by mass spectrometry as a ROC1-interacting protein. CUL7 is a large polypeptide containing a cullin domain, which is responsible for ROC1 binding, and a DOC domain, which is also present in the anaphase-promoting complex. Remarkably, CUL7 assembles an SCF-ROC1-like E3 ubiquitin ligase complex consisting of Skp1, CUL7, the Fbx29 F-box protein, and ROC1. In contrast to CUL1 that binds Skp1 by itself, CUL7 interacts with the Skp1·Fbx29 complex, but not with Skp1 alone. Strikingly, CUL7 selectively interacts with Skp1·Fbx29 but not with Skp1·βTRCP2 or Skp1·Skp2. Thus, CUL7 may define a previously uncharacterized, Fbx29-mediated, and ubiquitin-dependent proteolysis pathway.

Cullins are a family of structurally related proteins that share a C-terminally located, evolutionarily conserved cullin domain (1, 2). It is well established that several members of the cullin family are required for ubiquitin (Ub)-dependent proteolysis. CUL1, a subunit of the SCF-ROC1 E3 Ub ligase complex, contains distinct N- and C-terminal regions responsible for binding to the Skp1·F-box protein complex and to the ROC1 RING finger protein (also called Rbx1 or Hrt1), respectively (3, 4). In this manner, CUL1 places an F-box protein (member of a large family of substrate-targeting molecules) within the proximity of ROC1, which recruits an E2-conjugating enzyme (5–7). Consequently, a substrate, once bound to the F-box protein, is positioned optimally for accepting a Ub moiety in an E2-catalyzed transfer reaction. The CUL1-dependent SCF-ROC1 pathways target a wide variety of substrates including those involved in the control of DNA replication, transcription, cell cycle transition, and signal transduction (ref. 8 and references therein), thereby promoting unidirectional alteration of a divergent array of cellular processes.

In addition to its scaffolding role, CUL1 enhances the rate and efficiency with which SCF-ROC1 promotes ubiquitination, through the action of Nedd8 (reviewed in ref. 9). The covalent linkage between Nedd8 and CUL1 at residue K720 is predicted to position Nedd8 within close proximity of the E2-binding site in ROC1 (10). By utilizing its charged-surface residues, Nedd8 is thought to activate ubiquitination by mediating electrostatic interactions that increase the ability of ROC1 to promote the formation of multi-Ub chains (11, 12), presumably by facilitating the recruitment of an E2 (13).

CUL2 forms an E3 Ub ligase complex similar to SCF-ROC1, allowing the von Hipple-Lindau tumor suppressor protein to target proline-hydroxylated hypoxia-inducible factor for ubiquitination (ref. 14 and references therein). APC2, another well known cullin protein, is a component of the anaphase-promoting complex (APC) that regulates mitosis by targeting mitotic cyclins and securin for degradation (15). Intriguingly, APC2 binds the APC11 RING finger protein (a ROC1 homologue) in a manner analogous to the interaction between CUL1 and ROC1 (16). The precise cellular functions of mammalian CUL3, CUL4A/4B, and CUL5 remain to be determined.

Deletion and site-directed mutagenesis studies demonstrated that the cullin domain is essential for the interaction between CUL1 and ROC1 (4, 17, 18). Recent x-ray crystallographic studies revealed extensive contacts between multiple β-strands within the CUL1 cullin domain and the ROC1/Rbx1 N-terminal β-strand (10). Moreover, residues involved in ROC1 binding are highly conserved in CUL1 orthologues as well as in its paralogues. Sequence and structural analyses further suggest that besides CUL1, other cullin proteins may bear an N-terminally located site for binding to a Skp1-like adapter. These studies are consistent with the original hypothesis that mammalian cullins 3–5 as well as APC2 may resemble CUL1 and CUL2 in acting as molecular scaffolds, assembling both substrate targeting and core Ub ligase modules to mediate a ubiquitination reaction (16, 19).

In this study, we report the identification of a previously uncharacterized cullin, CUL7 (formally known as KIAA0076). Remarkably, CUL7 assembles an SCF-ROC1-like E3 ligase complex, consisting of Skp1, CUL7, Fbx29, and ROC1. However, CUL7 specifically interacts with Skp1·Fbx29, but not with Skp1 alone, Skp1·βTRCP2, or Skp1·Skp2, thereby demonstrating a striking selectivity of this molecular scaffold for assembling a putative Fbx29-based E3 Ub ligase complex.

Materials and Methods

Construction of Plasmids. ***Generation of pCR3.1-Flag-CUL7.*** Initially, the first 1,764 bp of CUL7 was amplified by PCR by using the pBlskII-ha00936 plasmid as the template. The following primers were used: 5′ primer (DD28)-GCCATATGACCATG**GATTACAAGGATGACGACGATAAG**GGATCCATGGTGGGAGAACTCCGCTAC (Flag tag is boldfaced); and 3′ primer (DD31)-CGCATATGGCGGCCGCCTAATCTTCTTGGGCTTCTAGAAGGG. The resulting PCR product was cloned into the pCR3.1-Uni vector (Invitrogen), creating pCR3.1-Flag-CUL7 (1–588 amino acids). In the second step, the entire CUL7 coding sequence, excluding the first 25 bp, was excised from the pBlkII-ha00936 plasmid by digestion with restriction enzymes *Eco*RI and *Not*I. The resulting fragment was then inserted into the pCR3.1-Flag-CUL7 (1–588aa) vector that previously had been digested with *Eco*RI and *Not*I to contain only the first 25 bp of the CUL7 sequence, creating pCR3.1-Flag-CUL7.

Generation of pCR3.1-Myc-Fbx29. The Fbx29 cDNA was obtained from a human fetal kidney cDNA library (CLONTECH) by PCR. The primers used are: 5′ primer (DD48)-GGCGGCCGCGAATTCGGACTGTCTCGTGGCACCCGG; and 3′ primer (DD51)-CCTCGAGCTAAACATGGTTATAGGGAAAGGCC. The primers were designed based on the Fbx29 sequence available in the GenBank database (accession no. AF176707).

Abbreviations: Ub, ubiquitin; APC, anaphase-promoting complex.

‡To whom correspondence should be addressed. E-mail: zhen-qiang.pan@mssm.edu.

BIOCHEMISTRY

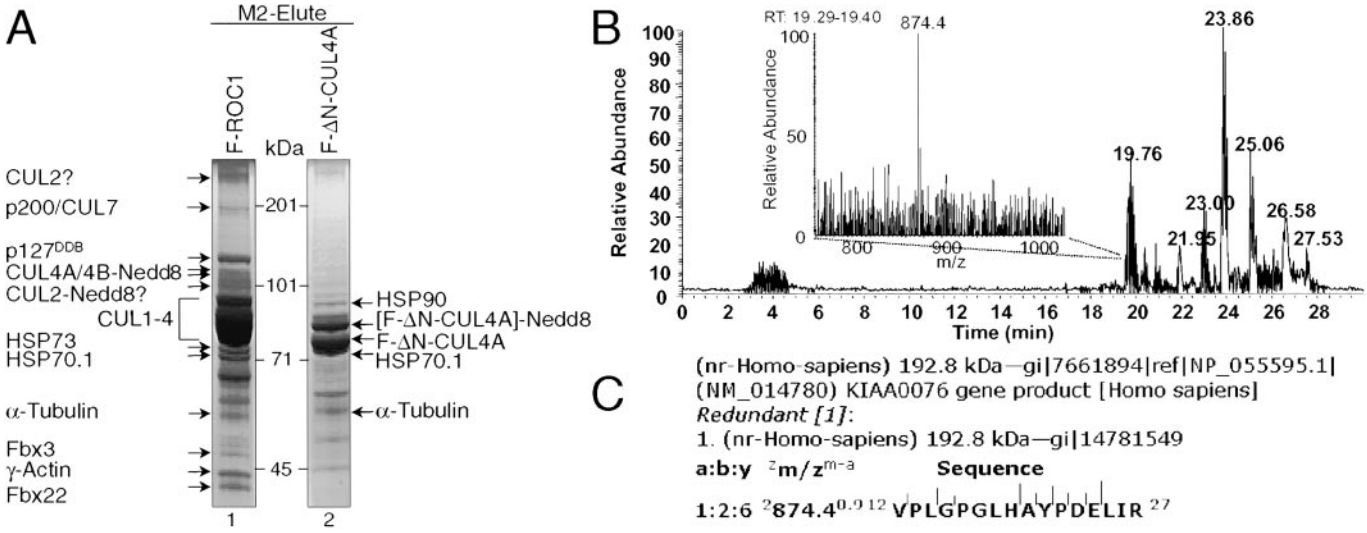

Fig. 1. Identification of CUL7 as a ROC1-interacting protein. (*A*) Coomassie stain analysis of the Flag-ROC1 immunoprecipitates. Flag-peptide eluants derived from ≈20 150-mm plates' worth of cells expressing either Flag (F)-ROC1 (lane 1) or Flag (F)-ΔN-CUL4A (lane 2) were concentrated by TCA precipitation followed by electrophoresis through SDS/10% PAGE and Coomassie staining. (*B* and *C*) Identification of p200 as CUL7 (KIAA0076) by micro-HPLC/electrospray ionization ion trap (ESI-IT)-MS/MS analysis. p200-derived tryptic peptides were fractionated by micro-C18–HPLC; the elution profile is shown in *B*. The insertion in *B* is an MS spectrum showing the detection of a peptide ion with m/z 874.4. Database searches using the entire p200 MS/MS data resulted in the identification of KIAA0076 gene product, shown in *C*. A detailed description of the MS/MS analysis can be found in the supporting information.

The resulting PCR product was used as the template for a second PCR, which was carried out by using DD51 as the 3′ primer and a Myc tag sequence (boldface)-containing 5′ primer (DD52-CGACCATG**GAGCAAAAGCTCATCTCAGAGGAGG-ATCTC**GAATTCGGACTGTCTCGTGGCACCCGG), and the resulting product was subcloned into the pCR3.1-Uni vector, creating pCR3.1-Myc-Fbx29. This vector yields a truncated Fbx29 protein that initiates with a glycine residue, lacking the extreme N terminus (Fig. 7, which is published as supporting information on the PNAS web site, www.pnas.org). However, given that this N-terminally truncated Fbx29 has a calculated molecular mass of 62.4 kDa, a value very close to the observed molecular mass for the p64/Fbx29 endogenous protein (for example, see Fig. 4*A*), we estimate that the truncation is less than 20 amino acid residues. In addition, there are discrepancies between our Fbx29 clone and the GenBank database sequence (accession no. AF176707), in the positions 236–249 (NIWDL-RTGKYPVHR, our clone; IFGIKDRKVPCSS, accession no. AF176707), as well as at amino acid 464 (E, our clone; K, accession no. AF176707). Database searches revealed that sequences derived from several human and mouse EST clones (accession nos. BQ425940, BE514576, AW402026, XM-084794, AL520439, BC009095, and AI425689) are in agreement with our clone with respect to the above-mentioned regions.

Procedures for generating other plasmids, stable cell lines, and anti-CUL7 antibody, for protein affinity purification and MS/MS analysis, as well as for other standard techniques, are described in *Supporting Materials and Methods*, which is published as supporting information on the PNAS web site.

Results

Identification of CUL7 as a ROC1-Bound Cullin Protein. In an attempt to identify previously uncharacterized ROC1 interacting proteins, we generated a cell line (293FR) constitutively expressing ROC1 with an N-terminal Flag epitope (Flag-ROC1). Coomassie staining analysis of components of the affinity-purified Flag-ROC1 complexes, separated by denaturing polyacrylamide gels, identified several proteins that were specifically associated with ROC1 (Fig. 1*A*). One such protein, p200 (lane 1), when analyzed by mass spectrometric peptide fragmentation (MS/MS), was found to contain a tryptic peptide whose mass value (1,746.81) as well as MS/MS peptide fragmentation spectrum matched the predicted mass of a KIAA0076-derived peptide, 1,745.95 (Fig. 1 *B* and *C*). This result suggests that p200 is identical to the gene product of *KIAA0076*. The *KIAA0076* cDNA was predicted to encode for an uncharacterized protein of 1,698 amino acids (20), with a theoretical molecular mass of 192.8 kDa (Fig. 1*C*), which contains a well documented cullin domain (Fig. 2). In accordance with the current nomenclature for cullin proteins, we herein designate KIAA0076 as CUL7, because a homologue of CUL1 in *Caenorhabditis elegans* has recently been named CUL6 (21).

Further sequence analysis revealed that CUL7 shares extensive homology with another large cullin domain-containing protein, KIAA0708 (Fig. 2) and is also related to HERC2, a putative *hect* E3 that may be associated with the Prader-Willi and Angelman syndromes (22). These three proteins all contain a DOC domain, located near the central region of CUL7 (Fig. 2), which was originally found in the APC10/DOC1 subunit of the APC E3 Ub ligase complex (23). Crystallographic analysis of APC10/DOC1 implicated a role for the jellyroll-shaped DOC domain in binding to ligands, such as sugars, nucleotides, phospholipids, DNA, and proteins (24), suggesting that the four

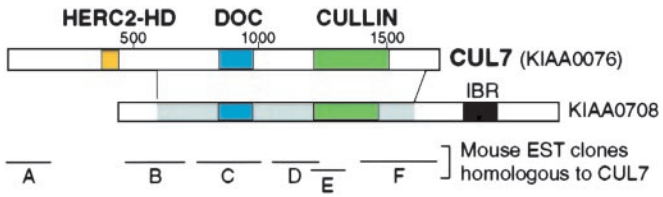

Fig. 2. Structural domains within CUL7. Structural similarity between CUL7 and KIAA0708 is indicated. HERC2-HD refers to a CUL7 N-terminal region that spans 72 amino acids, is enriched with glycine and acidic residues, and shares 59% similarity to the corresponding sequences in HERC2. IBR represents an in-between RING finger domain. Segments A–F are representative mouse EST clones [GenBank database accession nos. BB612579 (A), BG867165 (B), AW106876 (C), BG087524 (D), BF144723 (E), and BG078363 (F)] that are highly homologous to CUL7.

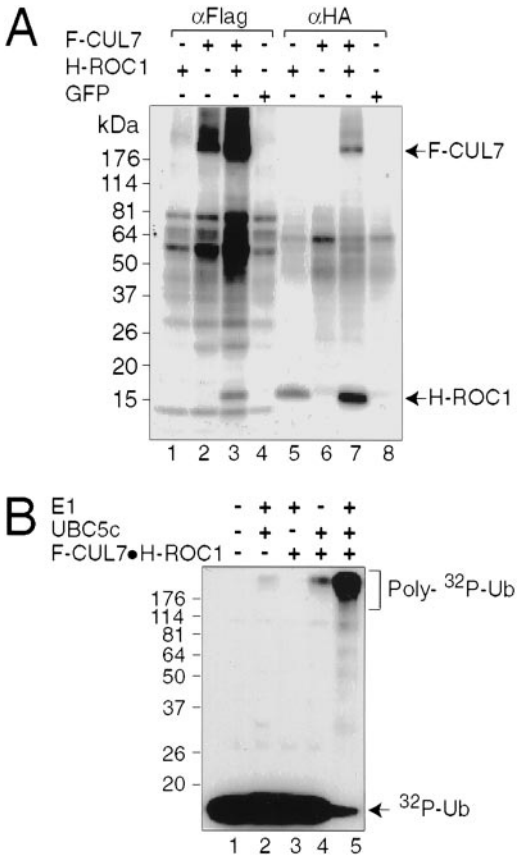

Fig. 3. CUL7 forms a complex with ROC1 that supports Ub polymerization. (*A*) CUL7 interacts with ROC1. Cells (293T) were transfected with pCR3.1-Flag (F)-CUL7 and/or pcDNA-HA (H)-ROC1 as indicated. ^{35}S-labeled extracts (≈3 mg of protein) were immunoprecipitated with αFlag (lanes 1–4) or αHA (lanes 5–8) antibodies, and the resulting immunoprecipitates were separated by SDS/4–20% PAGE followed by autoradiography. The identities of the polypeptides of molecular masses ranging from 50 to 80 kDa present in the anti-Flag immunoprecipitates (lanes 2 and 3) are presently unknown. (*B*) The CUL7·ROC1 complex supports ubiquitin polymerization. The Flag (F)-CUL7·HA (H)-ROC1 complex, immobilized onto the M2 beads, was analyzed for ubiquitin ligase activity as described (4). The autoradiogram is shown.

divergent E3 Ub ligases containing APC10, HERC2, CUL7, and KIAA0708 may be regulated similarly by a ligand-mediated mechanism.

Several additional points were revealed by mass spectrometric analysis of the ROC1-associated polypeptides. First, as expected, cullins 1–4 were the most abundant species that copurified with ROC1 (Fig. 1*A*, lane 1). In contrast, only low levels of CUL7 were detected in the Flag-ROC1 immunoprecipitates, suggesting that this protein is less abundant than other cullins. Surprisingly, the largest protein with an apparent molecular mass of ≈300 kDa appeared to contain at least two peptides that matched the sequence of CUL2. However, the identity of this large "CUL2" species remains to be determined.

Next, we determined whether CUL7 interacted with ROC1 in transiently transfected 293T cells. Immunoprecipitation of extracts containing metabolically ^{35}S-labeled Flag-CUL7 and HA-ROC1 copurified the two components (Fig. 3*A*, lanes 3 and 7). This association was not detected in cells that only expressed Flag-CUL7 (lanes 2 and 6), HA-ROC1 (lanes 1 and 5), or GFP (lanes 4 and 8), demonstrating the specificity of the ROC1–CUL7 interaction. Identical results were obtained with immunoprecipitation/immunoblot experiments (data not shown). Further, we tested whether the CUL7·ROC1 complex was active in assembling polyubiquitin chains in an E1/E2-dependent manner, a property common to a large number of ROC1–cullin complexes (19, 25). The result showed that the immunopurified Flag-CUL7·HA-ROC1 complex, when incubated with E1 and Ubc5c, converted the majority of monomeric [^{32}P]-Ub into high molecular weight Ub conjugates (Fig. 3*B*, lane 5). The observed Ub polymers likely include both free Ub chains (4) and auto-ubiquitinated E2 (5). Omission of E1 (lane 4), Ubc5c (lane 3), or Flag-CUL7·HA-ROC1 (lane 2) abolished the reaction, demonstrating that CUL7 is capable of forming a complex with ROC1 that supports Ub polymerization.

In summary, we identified a previously uncharacterized ROC1-interacting protein, CUL7, which contains both the cullin and the DOC signature domains. Mammalian cullins 1–5 and APC2 are similar in size, with molecular masses in the range of 80–90 kDa, and have orthologues in lower eukaryotes. In contrast, CUL7, with a molecular mass greater than 190 kDa, although conserved in mammals (Fig. 2), may not have homologues in lower species, as revealed by database search analysis, thus implicating a specific role for this cullin in higher eukaryotes.

CUL7 Assembles an SCF-ROC1-Like Complex That Contains Skp1 and Fbx29. A stable cell line (293FC7) that constitutively expresses CUL7 with an N-terminal Flag epitope (Flag-CUL7) was created to facilitate isolation of the native CUL7 complex. To identify components that associate with CUL7 in a stoichiometric manner, the affinity-purified Flag-CUL7 complex was analyzed by gel filtration using Superdex-200. The results of silver staining (Fig. 4*A Upper*) and immunoblot (*Lower*) analyses revealed that the Flag-CUL7 protein peaked between fractions 14 and 16, coincidental with the peak of the endogenous ROC1 protein (Fig. 4*A Upper* and *Lower*, lanes 4–6), thereby supporting the notion that these two components interact. Intriguingly, two distinct polypeptides with apparent molecular masses of 19 and 64 kDa, p19 and p64, respectively, comigrated with Flag-CUL7 and ROC1 (Fig. 4*A Upper*, lanes 4–6). Moreover, it appeared that Flag-CUL7, ROC1, p19, and p64 were present in near stoichiometric amounts, suggesting that like ROC1, both p19 and p64 are integral components of the native CUL7 complex.

Further mass spectrometry analysis showed that the masses of three peptides derived from p19 matched predicted mass values of three Skp1 peptide sequences (Fig. 7*A*). Subsequent immunoblot analysis confirmed the identity of p19 as Skp1 (Fig. 4*A Lower*). p64 most likely corresponds to the gene product of *Fbx29*, as eight p64-derived peptides possessed identical mass values to those predicted for this uncharacterized WD40 repeat-containing F-box protein (Fig. 7*B*). Furthermore, immunoprecipitation of 293 cell extracts with anti-CUL7 antibody revealed that the endogenous CUL7 was associated with Skp1 and ROC1 (Fig. 4*B*). Because of an unavailability of anti-Fbx29 antibodies, the presence of Fbx29 in the anti-CUL7 immunoprecipitates could not be determined. Taken together, these data strongly suggest that CUL7 interacts with ROC1, Skp1, and Fbx29 to form an SCF-like E3 Ub ligase complex.

CUL7 Selectively Interacts with the Skp1·Fbx29 Complex. Transient transfection experiments were carried out to verify the interactions between CUL7, Skp1, and Fbx29. When overexpressed in 293T cells, Flag-CUL7, Skp1-HA, Myc-Fbx29, and Flag-ROC1 formed a complex that was immunoprecipitated by anti-Myc antibodies (Fig. 5*A*, lane 1). In the absence of Skp1-HA, Myc-Fbx29 formed a complex with Flag-CUL7, endogenous Skp1, and ROC1, in either recombinant or native forms (lane 3). As expected, high levels of Skp1-HA were coimmunoprecipitated with Myc-Fbx29 independently of the presence of Flag-CUL7 (lane 4). Note that low levels of endogenous ROC1 were also coimmunoprecipitated by the anti-Myc antibodies in the

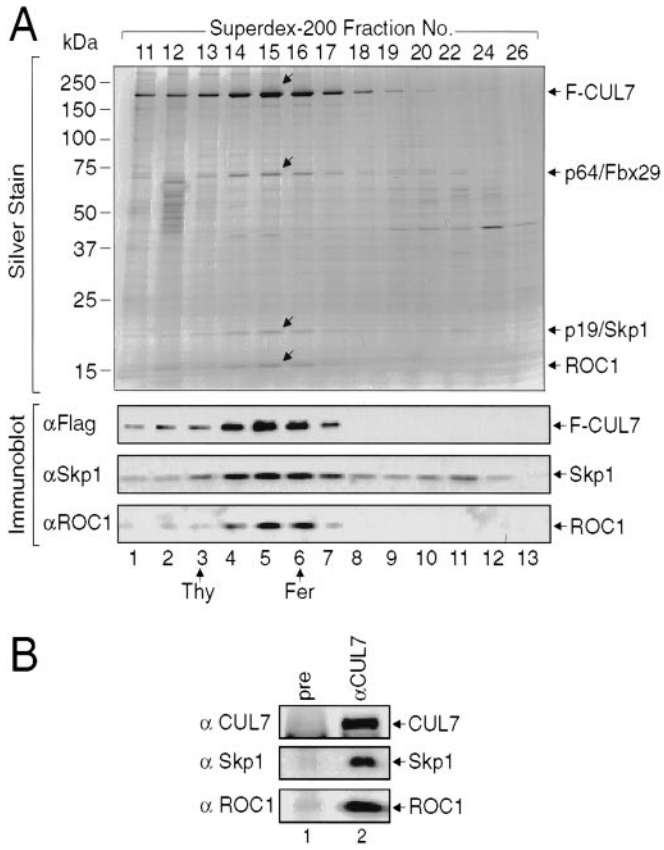

Fig. 4. Identification of the CUL7·Skp1·Fbx29·ROC1 complex. (*A*) Comigration of CUL7, ROC1, p19, and p64 upon Superdex-200 gel filtration. The Flag-peptide eluant containing Flag (F)-CUL7 and its associated proteins was separated by gel filtration on a Superdex-200 column, as described in the supporting information. Aliquots of the indicated fractions (12 μl) were electrophoresed on 4–20% gradient denaturing gels and analyzed by silver staining (*Upper*) and by immunoblotting by using antibodies as indicated (*Lower*). Arrows at the bottom denote the positions where size markers thyroglobulin (Thy, 669 kDa) and ferritin (Fer, 440 kDa) migrated. (*B*) Association of endogenous CUL7 with Skp1 and ROC1. Preimmune or anti-CUL7 serum, 100 μl each, was prebound to protein A agarose beads (15 μl) overnight at 4°C, followed by an extensive wash. The resulting beads then were mixed with extracts of 293 cells (≈72 mg of protein), and the mixture was rocked overnight at 4°C. After washing, the immunopurified proteins were eluted from the beads and analyzed by immunoblotting using antibodies as indicated.

absence of Flag-CUL7 (lane 4), most likely because of the bridging effect of endogenous CUL7 or CUL1 proteins that connect ROC1 and Skp1·Fbx29 (see Fig. 6). As shown, similar levels of Myc-Fbx29, Flag-CUL7, or Skp1-HA were present in the transfected cells analyzed (compare the second, sixth, and seventh panels from top). Additionally, Myc-immunoprecipitates derived from cell extracts containing Flag-CUL7, Skp1, Myc-Fbx29, and ROC1 contained a Ub ligase activity (Fig. 8, which is published as supporting information on the PNAS web site). Thus, CUL7, ROC1, Skp1, and Fbx29 interact to form an SCF-like functional complex.

Surprisingly, in the absence of Myc-Fbx29, Flag-CUL7 did not form a complex with Skp1 in either its recombinant or native forms (Fig. 5*B*, compare lanes 1 and 2 in the second, third, and fourth panels from top). Note that comparable amounts of Flag-CUL7 and Skp1-HA were present in cells that expressed or did not express Myc-Fbx29 (Fig. 5*B*, compare lane 1 and lane 2 in the first and seventh panels from top). This result demonstrated a fundamental difference between CUL7 and CUL1, the latter of which did not require an F-box protein to efficiently interact with Skp1 (Fig. 5*C*, compare lanes 1 and 2 with lanes 3 and 4; also see ref. 26). However, Skp1 was still required for the efficient association between CUL7 and Fbx29, as removal of the Skp1-interacting F-box motif significantly impaired the ability of Fbx29 to interact with CUL7 (Fig. 5*D*, compare lanes 1 and 2, *Middle*; lanes 4 and 5, *Top*). These data strongly suggest that CUL7 efficiently interacts with the Skp1·Fbx29 complex, but not with either alone.

Of note, although no detectable Skp1 was present in the Flag-CUL7 immunoprecipitates by the M2-antibody in the absence of Myc-Fbx29 (Fig. 5*B*, lane 2), anti-CUL7 antibody coimmunoprecipitated the endogenous CUL7, ROC1, and Skp1 (Fig. 4*B*). It is possible that the endogenous Fbx29 and/or Skp1·Fbx29 are not present in cells at a level that is sufficient for an interaction with transiently expressed Flag-CUL7. However, the endogenous CUL7 may form a complex with cellular Fbx29, Skp1, and ROC1, as suggested by the immunoprecipitation experiment shown in Fig. 4*B*.

Next, we determined whether CUL7 selectively interacted with the Skp1·Fbx29 complex by comparing Fbx29 to βTRCP2 (a WD40 repeat-containing F-box protein, also called HOS) and to Skp2 (a leucine-rich F-box protein) for their ability to associate with either CUL7 or CUL1 in transfected 293T cells. As shown, Myc-Fbx29 efficiently formed a complex with Flag-CUL7 (Fig. 6*A Bottom*, lane 1 and *Top*, lane 4). Notably, the amount of Myc-Fbx29 in the Flag-CUL7 immunoprecipitates was comparable to that observed with the anti-Myc-Fbx29 immunoprecipitation (compare Fig. 6*A Bottom,* lanes 1 and 4), indicating that Myc-Fbx29 was almost quantitatively associated with Flag-CUL7. These results demonstrated a remarkable efficiency with which CUL7 interacted with Skp1·Fbx29. Of note, only a fraction of Flag-CUL7 was complexed with Myc-Fbx29 (compare lanes 1 and 4, *Top*). This result most likely reflected the presence of excess amounts of the recombinant CUL7 protein, relative to Myc-Fbx29, in transiently transfected cells.

The association between Flag-CUL1 and Myc-Fbx29 was much less efficient in comparison to Flag-CUL7 (compare Fig. 6*A Bottom,* lanes 1 and 2; compare *Top*, lanes 4 and 5), despite the presence of comparable amounts of these proteins (for Flag-CUL7 and Flag-CUL1, compare Fig. 6*A Top* lanes 1 and 2; for Myc-Fbx29, compare *Bottom*, lanes 4 and 5). In contrast, HA-βTRCP2 (Fig. 6*B*) or Myc-Skp2 (Fig. 6*C*) efficiently formed a complex with Flag-CUL1, but not with Flag-CUL7. As noted, nearly 50% of HA-βTRCP2 or Myc-Skp2 was associated with Flag-CUL1 (Fig. 6 *B* or *C*, compare lanes 2 and 5), an indication of an efficient association between these components. In conclusion, CUL7 exhibits a higher affinity than CUL1 for interaction with the Skp1·Fbx29 complex, but not for Skp1 alone. Unlike CUL1, CUL7 interacts with neither Skp1·βTRCP2 nor Skp1·Skp2. Thus, these studies establish CUL7 as a unique cullin protein that selectively assembles a putative Fbx29-based E3 Ub ligase complex.

Discussion

Based on studies presented in this paper, we propose that CUL7 functions as a molecular scaffold specifically for Fbx29, setting a foundation for a previously uncharacterized Ub-dependent protein degradation pathway.

We have provided compelling biochemical evidence demonstrating that CUL7 assembles an SCF-ROC1-like complex, consisting of Skp1, CUL7, Fbx29, and ROC1. First, the recombinant CUL7 formed a near stoichiometric complex with endogenous Fbx29, Skp1, and ROC1 in 293FC7 cells (Fig. 4*A*). In addition, immunoprecipitation experiments revealed the association between endogenous CUL7, Skp1, and ROC1 (Fig. 4*B*). Moreover, coexpression of recombinant CUL7, ROC1, Skp1,

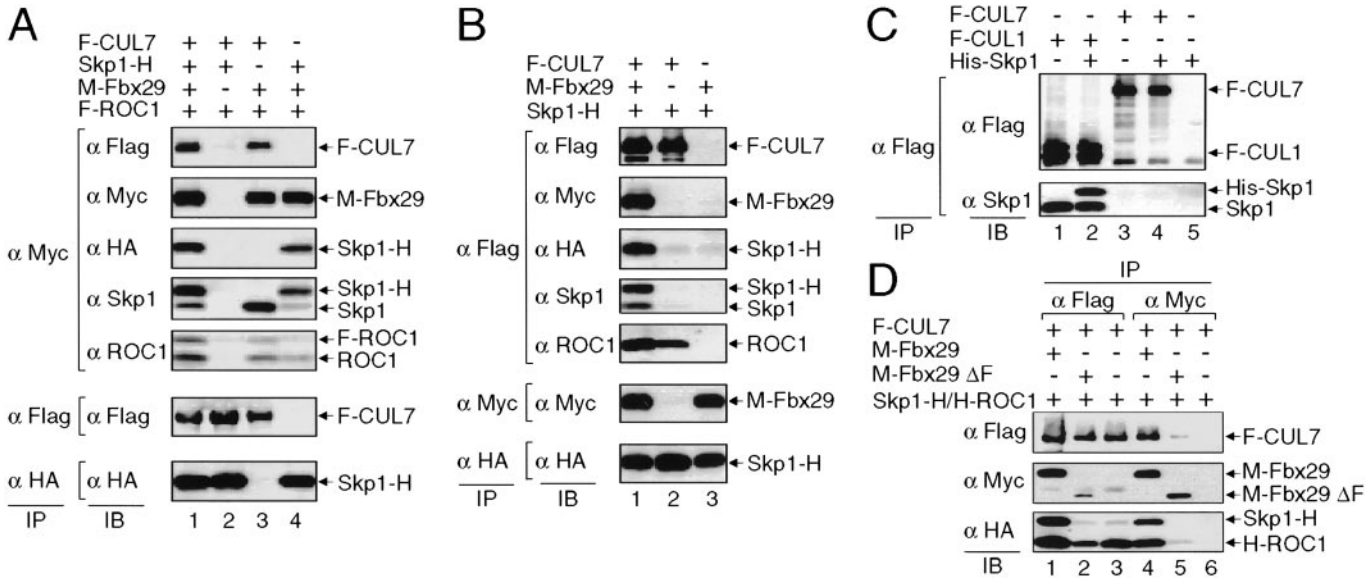

Fig. 5. CUL7 binds Skp1·Fbx29 but not Skp1 alone. Cells (293T) were cotransfected with an indicated set of vectors expressing Flag (F)-CUL7, Flag (F)-CUL1, Skp1-HA (H), His-Skp1, Myc (M)-Fbx29, Myc (M)-Fbx29 ΔF, Flag (F)-ROC1, or HA (H)-ROC1. Protein extracts (10 mg) were immunoprecipitated by anti-Myc, anti-Flag, or anti-HA antibodies, as indicated. The resulting immunoprecipitates were analyzed by immunoblots by using the specified antibodies.

and Fbx29 led to the formation of the four-subunit complex in 293T cells (Fig. 5). Initial gel filtration analysis of the purified Flag-CUL7·Skp1·Fbx29·ROC1 complex yielded a Stokes radius consistent with that of a globular complex of 440 kDa (Fig. 4*A*). However, if CUL7 structurally resembles CUL1, which adopts an extremely elongated shape (10), the CUL7·Skp1·Fbx29·ROC1 complex is expected to migrate in a manner that is very different from the globular shaped-assembly (27). Thus, a more extensive analysis is required to determine accurately the molecular mass and stoichiometry of this complex.

Remarkably, in a manner strikingly different from CUL1 that binds Skp1 in the absence of an F-box protein (Fig. 5*C*, and ref. 26), CUL7 interacted with the Skp1·Fbx29 complex, but not with Skp1 alone (Fig. 5*B*). Most interestingly, CUL7 exhibited a marked selectivity in that it efficiently formed a complex with Skp1·Fbx29 but not with Skp1·βTRCP2 or Skp1·Skp2 (Fig. 6). Furthermore, CUL7 had a higher affinity than CUL1 for binding to the Skp1·Fbx29 complex (Fig. 6*A*). This notion was further substantiated by observations that in the 293FC7 cells, Fbx29 was the only endogenous F-box protein detected that formed a near stoichiometric complex with the recombinant CUL7 (Fig. 4*A*). By contrast, Fbx3 and Fbx22, but not Fbx29, were the two most abundant F-box proteins that formed complexes with CUL1 (Fig. 1*A*; and data not shown). Taken together, these results demonstrate that CUL7 selectively interacts with the Skp1·Fbx29 complex to assemble a putative Fbx29-based E3 Ub ligase.

How does CUL7 form a complex with Skp1·Fbx29? We hypothesize that Fbx29 contains an element that is absent in other F-box proteins such as βTRCP2 or Skp2 but which critically contributes to the interaction between CUL7 and

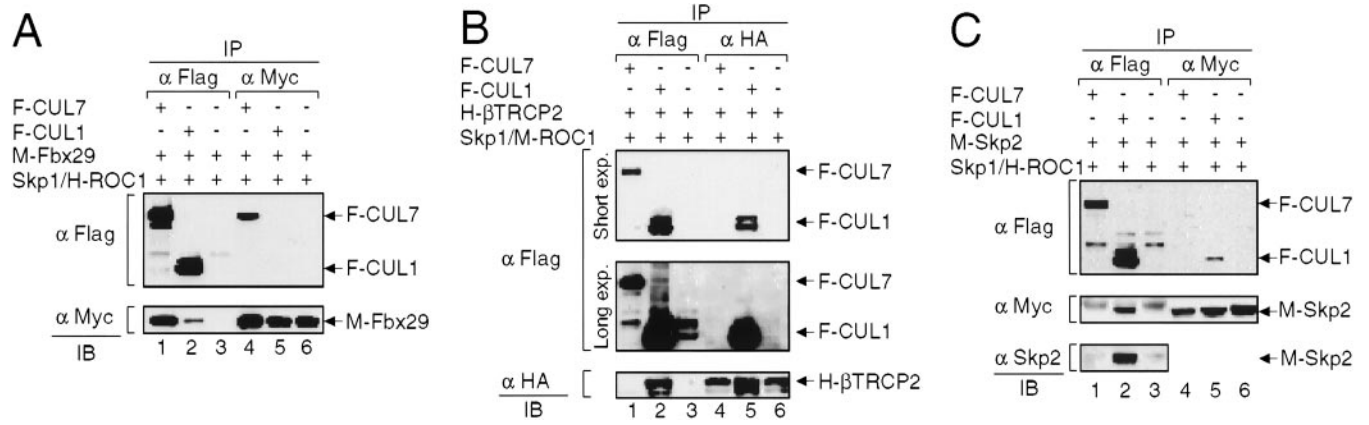

Fig. 6. Selective interaction between CUL7 and Skp1·Fbx29. For comparison, pCR3.1-Flag (F)-CUL7 (lanes 1 and 4) or pCR3.1-Flag (F)-CUL1 (lanes 2 and 5) were cotransfected with pCR3.1-Myc (M)-Fbx29 (*A*), pcDNA-HA (H)-βTRCP2 (*B*), or pcDNA-Myc (M)-Skp2 (*C*), along with pcDNA-Skp1 and pcDNA-HA (H)-ROC1 or pcDNA-Myc (M)-ROC1. Immunoprecipitates were analyzed by Western immunoblotting by using antibodies as specified. (*B*) The anti-Flag blot is shown with both long (*Middle*, 2-min) and short (*Top*, 15-s) exposures for better illustration of the inability of CUL7 to interact with Skp1·HA-βTRCP2. (*C*) Note that the Myc-Skp2 protein that was coimmunoprecipitated with Flag-CUL1 migrated slightly faster than the nonspecific IgG heavy chains (compare lane 2 with lanes 1 and 3, *Middle*). In addition, anti-Skp2 immunoblot of the Myc immunoprecipitates is not shown. For unknown reasons, anti-Skp2 antibodies used in this study exhibited unusually high levels of nonspecific interactions with the heavy chains of Myc antibodies, which comigrated with the Myc-Skp2 proteins, thereby precluding the evaluation of Myc-Skp2 in the immunoprecipitates.

Skp1·Fbx29. Based on the observations that Skp1 was incapable of interacting with CUL7 by itself (Fig. 5*B*), yet was required for the efficient CUL7-Fbx29 association (Fig. 5*D*), this adapter protein probably acts to stabilize the CUL7·Skp1·Fbx29 ternary complex. Given that CUL1 inefficiently interacted with Skp1·Fbx29, Fbx29 must form a complex with Skp1 in a manner that is substantially different from βTRCP2 or Skp2. In the CUL1·Skp1·Skp2 interaction model, the leucine-rich region of Skp2 is not predicted to be within contact distance of Skp1 or CUL1 (10). Possibly, the WD40 repeat region of Fbx29 (Fig. 7*B*) is arranged in such a way that it may provide considerable structural restraints that prevent an efficient interaction between CUL1 and Skp1·F-box^{Fbx29}.

There seems to be a precedent case in which a Skp1·F-box protein subcomplex is assembled into an E3 ligase in a CUL1-independent manner. Matsuzawa and Reed (28) have shown that the Siah-1 RING finger protein is associated with Skp1·Ebi (an F-box protein) via SIP that interacts with both Siah-1 and Skp1. Intriguingly, SIP selectively binds Skp1·Ebi but not Skp1·βTRCP, which is reminiscent of CUL7 in its specific binding to Skp1·Fbx29 (Fig. 6). However, SIP interacts with Skp1 directly (28), whereas CUL7 forms a complex with Skp1 only in the presence of Fbx29 (Fig. 5*B*). It should be pointed out that whether Skp1·Ebi interacts with the CUL1·ROC1 complex has not been examined, as such an interaction could form an SCF^{Ebi}-ROC1 E3 Ub ligase directing β-catenin degradation in a Siah-1-independent fashion.

Conceptually, the present study further underscores and extends the combinatorial nature of the SCF-ROC1 E3 ligases. It now seems that three components of this type of E3 complex, the F-box protein, the Skp1 adapter, as well as the cullin scaffold, are all interchangeable. It is well established that many members of the large F-box protein family become associated with Skp1·CUL1·ROC1 through their interactions with Skp1, via the F-box domain. At least in *C. elegans*, various Skp1-related gene products exist, and some of these show differential interactions with F-box proteins (29). This observation suggests that by virtue of their selective interactions with a subset of F-box proteins, Skp1-related proteins may define specificity in assembly of SCF-ROC1 complexes. The current study provides an example in which the CUL1 subunit can also be replaced, in this case by CUL7, which selectively interacts with Skp1·Fbx29 to form an SCF-ROC1-like complex. Furthermore, our analysis demonstrates that the binding of Skp1 to an F-box protein, such as Fbx29, results in a "gain of a function," allowing the complex to interact with CUL7. This provocative finding invites reinvestigation of the interaction between Skp1 and cullins. Although it is true that only CUL1 binds Skp1 alone (26), it cannot be excluded that other cullin proteins may bind to some unique Skp1·F-box protein complexes, in a manner analogous to the observed interaction between CUL7 and Skp1·Fbx29.

Ub-dependent degradation of cellular regulatory proteins mediated by F-box family members plays critical roles in cell biology. Whereas CUL1 serves as a molecular bridge that likely connects a large number of F-box proteins to an E2-conjugating enzyme through ROC1, the current study demonstrates that CUL7 functions as an alternative scaffold, at least for Fbx29, owing to its ability to selectively interact with the Skp1·Fbx29 complex. Hence, mechanisms used by F-box proteins to assemble E3 ligases capable of targeting substrates for ubiquitination may vary, presumably reflecting their varying physiological functions.

We thank T. Ohta and M. Pagano for reagents; V. Bermudez for assistance in gel filtration analysis using Superdex 200 PC 3.2/30; J. Hurwitz for helpful discussion; P. Cortes and J. Mansilla-Soto for guidance in the generation of stable cell lines; S. Santagata for critical reading of the manuscript; and the Kazusa DNA Research Institute, Japan, for the KIAA0076 cDNA. This study was supported by Public Health Service Grant GM61051 (to Z.-Q.P.). D.C.D. was supported by a predoctoral fellowship from the Portuguese Foundation for Science and Technology (Praxis XXI/BD/13442/97) and by a grant from the Peter Sharp Foundation. R.W. is supported by National Institutes of Health Grant CA88325. Z.-Q.P. is an Irma T. Hirschl Scholar.

1. Zachariae, W., Shevchenko, A., Andrews, P. D., Ciosk, R., Galova, M., Stark, M. J., Mann, M. & Nasmyth, K. (1998) *Science* **279,** 1216–1219.
2. Yu, H., Peters, J.-M., King, R. W., Page, A. M., Hieter, P. & Kirschner, M. W. (1998) *Science* **279,** 1219–1222.
3. Patton, E. E., Willems, A. R., Sa, D., Kuras, L., Thomas, D., Craig, K. L. & Tyers, M. (1998) *Genes Dev.* **12,** 692–705.
4. Wu, K., Fuchs, S. Y., Chen, A., Tan, P., Gomez, C., Ronai, Z. & Pan, Z.-Q. (2000) *Mol. Cell. Biol.* **20,** 1382–1393.
5. Skowyra, D., Koepp, D. M., Kamura, T., Conrad, M. N., Conaway, R. C., Conaway, J. W., Elledge, S. J. & Harper, J. W. (1999) *Science* **284,** 662–665.
6. Seol, J. H., Feldman, R. M., Zachariae, W., Shevchenko, A., Correll, C. C., Lyapina, S., Chi, Y., Galova, M., Claypool, J., Sandmeyer, S., *et al*. (1999) *Genes Dev.* **13,** 1614–1626.
7. Chen, A., Wu, K., Fuchs, S. Y., Tan, P., Gomez, C. & Pan, Z.-Q. (2000) *J. Biol. Chem.* **275,** 15432–15439.
8. Deshaies, R. J. (1999) *Annu. Rev. Cell Dev. Biol.* **15,** 435–467.
9. Pickart, C. M. (2001) *Annu. Rev. Biochem.* **70,** 503–533.
10. Zheng, N., Schulman, B. A., Song, L., Miller, J. J., Jeffrey, P. D., Wang, P., Chu, C., Koepp, D. M., Elledge, S. J., Pagano, M., *et al.* (2002) *Nature* **416,** 703–709.
11. Wu, K., Chen, A. & Pan, Z.-Q. (2000) *J. Biol. Chem.* **275,** 32317–32324.
12. Wu, K., Chen, A., Tan, P. & Pan, Z.-Q. (2002) *J. Biol. Chem.* **277,** 516–527.
13. Kawakami, T., Chiba, T., Suzuki, T., Iwai, K., Yamanaka, K., Minato, N., Suzuki, H., Shimbara, N., Hidaka, Y., Osaka, F., *et al.* (2001) *EMBO J.* **20,** 4003–4012.
14. Conaway, R. C., Brower, C. S. & Conaway, J. W. (2002) *Science* **296,** 1254–1258.
15. Peters, J. M. (2002) *Mol. Cell* **9,** 931–943.
16. Ohta, T., Michel, J. J., Schottelius, A. J. & Xiong, Y. (1999) *Mol. Cell* **3,** 535–541.
17. Wirbelauer, C., Sutterluty, H., Blondel, M., Gstaiger, M., Peter, M., Reymond, F. & Krek, W. (2000) *EMBO J.* **19,** 5362–5375.
18. Furukawa, M., Zhang, Y., McCarville, J., Ohta, T. & Xiong, Y. (2000) *Mol. Cell. Biol.* **20,** 8185–8197.
19. Tan, P., Fuchs, S. Y., Chen, A., Wu, K., Gomez, C., Ronai, Z. & Pan, Z.-Q. (1999) *Mol. Cell* **3,** 527–533.
20. Nomura, N., Nagase, T., Miyajima, N., Sazuka, T., Tanaka, A., Sato, S., Seki, N., Kawarabayasi, Y., Ishikawa, K. & Tabata, S. (1994) *DNA Res.* **1,** 223–229.
21. Nayak, S., Santiago, F. E., Jin, H., Lin, D., Schedl, T. & Kipreos, E. T. (2002) *Curr. Biol.* **12,** 277–287.
22. Ji, Y., Walkowicz, M. J., Buiting, K., Johnson, D. K., Tarvin, R. E., Rinchik, E. M., Horsthemke, B., Stubbs, L. & Nicholls, R. D. (1999) *Hum. Mol. Genet.* **8,** 533–542.
23. Kominami, K., Seth-Smith, H. & Toda, T. (1998) *EMBO J.* **17,** 5388–5399.
24. Wendt, K. S., Vodermaier, H. C., Jacob, U., Gieffers, C., Gmachl, M., Peters, J. M., Huber, R. & Sondermann, P. (2001) *Nat. Struct. Biol.* **8,** 784–788.
25. Furukawa, M., Ohta, T. & Xiong, Y. (2002) *J. Biol. Chem.* **277,** 15758–15765.
26. Michel, J. J. & Xiong, Y. (1998) *Cell Growth Differ.* **9,** 435–449.
27. Johansson, E., Majka, J. & Burgers, P. M. (2001) *J. Biol. Chem.* **276,** 43824–43828.
28. Matsuzawa, S. I. & Reed, J. C. (2001) *Mol. Cell* **7,** 915–926.
29. Yamanaka, A., Yada, M., Imaki, H., Koga, M., Ohshima, Y. & Nakayama, K. I. (2002) *Curr. Biol.* **12,** 267–275.